Metasurface Polarization Optics: Phase Manipulation for Arbitrary Polarization Conversion Condition

Siqi Li,[1] Chen Chen,[2] Guoxi Wang,[1,3] Suyang Ge,[1,3] Jiaqi Zhao,[1,3] Xianshun Ming,[1] Wei Zhao,[1,3] Tao Li,[2,*] and Wenfu Zhang[1,3,†]

[1]*State Key Laboratory of Transient Optics and Photonics, Xi'an Institute of Optics and Precision Mechanics of Chinese Academy of Sciences, Xi'an 710119, China*

[2]*National Laboratory of Solid State Microstructures, Key Laboratory of Intelligent Optical Sensing and Manipulations, Jiangsu Key Laboratory of Artificial Functional Materials, College of Engineering and Applied Sciences, Nanjing University, Nanjing 210093, China*

[3]*University of Chinese Academy of Sciences, Beijing 100049, China*

(Received 29 February 2024; revised 5 November 2024; accepted 2 December 2024; published 14 January 2025)

Metasurface polarization optics have attracted considerable attention due to their ability to manipulate independently the wave fronts of different polarization channels with subwavelength scale. Previous methods mainly focused on the condition of complete polarization conversion, restricting the application range of metasurface polarization multiplexing. Here, we proposed a generalized framework of phase manipulation for the metasurface polarization optics, which can realize independent phase control and arbitrary energy distribution of different polarization channels for the arbitrary polarization conversion efficiency. Based on this principle, we experimentally demonstrate tripolarization-channel wavefront control for the arbitrary polarization state (elliptical, circular, and linear). The arbitrary energy distribution of different polarization channels has been achieved via varying the polarization conversion efficiency. The proposed framework significantly improves the performance of metasurface in the polarization multiplexing and energy distribution, and expands the application scope of metasurface in the polarization optics.

DOI: 10.1103/PhysRevLett.134.023803

Metasurfaces, consisting of an array of two-dimensional subwavelength metallic or dielectric nanostructures (meta-atoms), are a planar platform for manipulating the various fundamental properties of light such as the phase profile, polarization state, intensity distribution, and scattering angle on demand [1–6]. Recently, metasurface-based polarization optics has garnered significant attention for its breakthrough advantage in engineering multichannel independent wave front encoding due to the intimate relationship between the manipulated phase and the polarization state [7]. The propagation phase and geometric (or Pancharatnam-Berry, PB) phase are two basic mechanisms used for controlling the wave front of linear and circular polarization states [8,9]. Creatively, a phase regulation model based on hybrid of these two basic phases is proposed to realize independent phase control of arbitrary orthogonal polarizations [10]. This model paves a way for developing various polarization-dependent switchable nanodevices [11–13].

However, until now, much of the effort in the phase manipulation based on metasurface has primarily focused on the condition that the incident light is completely converted to its complex conjugate state (CCS) after passing through the metasurface [or ignoring the portion converted into its orthogonal complex conjugate state (OCS)] [14–17]. For example, the left-handed circularly polarized (LCP) light is converted to the right-handed circularly polarized (RCP) light with one phase, and the RCP light is converted to the LCP light with another phase [18,19]. Consequently, the number of polarizations multiplexing channels is limited to two or fewer based on independent phase control of arbitrary orthogonal states of polarization [20,21]. To break this capacity limit of polarization multiplexing, metasurfaces utilizing multiatom interference coupling or multilayer structures have been proposed [22–25]. However, these methods either reduce the spatial sampling rate, leading to a deterioration of the encoded information, or increase the number of layers in the metasurface, resulting in decreased manipulation efficiency. Recently, metasurface phase manipulation based on partial polarization conversion conditions has been reported, achieving three independent polarization multiplexing channels via a single-layer metasurface [26–29]. Nonetheless, these methods are only applicable to linear or circular polarization states and do not address the most general case: elliptical polarization state. Furthermore, all

*Contact author: taoli@nju.edu.cn

†Contact author: wfuzhang@opt.ac.cn

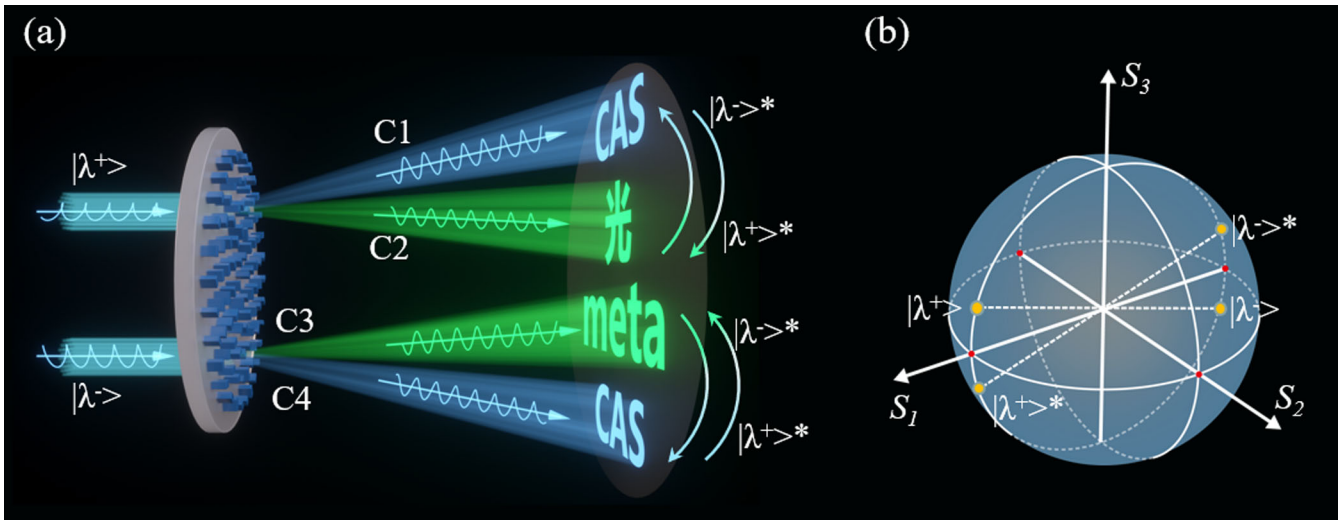

FIG. 1. (a) Conceptual schematic diagram of the proposed generalized framework for light manipulation. The independent phase manipulation for tripolarization channels can be realized based on the single-layer metasurface in the partial polarization conversion condition. The energy distribution of $C1$ and $C2$ ($C3$ and $C4$) can be effectively controlled by polarization conversion efficiency. (b) The position of the incident and transmitted polarization states on the Poincaré sphere.

the aforementioned methods fail to achieve energy regulation between different polarization multiplexing channels, which restricts the application range of metasurfaces.

Herein, we propose a generalized framework for phase manipulation in metasurface-based polarization optics, applicable to arbitrary polarization state and arbitrary polarization conversion efficiency. Utilizing this framework, both the independent phase and the arbitrary energy ratio of the component CCS and OCS in the transmission can be effectively manipulated by a single layer metasurface. For a pair of arbitrary orthogonally polarized incident light, the independent phase control of three polarization channels can be achieved with flexible energy distribution simultaneously. The proposed framework addresses the challenge of light manipulation under partial polarization conversion conditions, enhancing the performance of metasurfaces in polarization multiplexing and energy distribution, and exhibits significant potential for the development of multifunctional metadevices.

Figure 1(a) shows a schematic diagram for the proposed framework of phase manipulation based on metasurface. For arbitrary polarized light (noted as $|\lambda^+\rangle$) incident on the metasurface, it will be converted to two components $|\lambda^+\rangle^*$ and $|\lambda^-\rangle^*$ (states $|\lambda^+\rangle$ and $|\lambda^-\rangle$ are mutually orthogonal), shown in Fig. 1(b) due to the incomplete polarization conversion condition. These two components can be effectively manipulated with independent phase and arbitrary energy ratio. Here, the polarization conversion efficiency is defined as the ratio that the incident light is converted into its CCS. This applies equally to the incident polarized light $|\lambda^-\rangle$. For convenience, the polarization channels are noted as $C1$, $C2$, $C3$, and $C4$, respectively. As the information of channels $C1$ and $C4$ are the same (it will be demonstrated in the next), three polarization channels with independent phase manipulation can be achieved, which breaks through the limitation of polarization multiplexing channels of the model based on the complete polarization conversion condition. Besides, the energy ratio of $C1$ to $C2$ (or $C3$ to $C4$) can be controlled simultaneously by the metasurface, which provides a flexible manipulation of energy distribution for the metasurface-based polarization optics.

As is known, the unique properties of metasurface for polarization optics mainly originate from the local birefringence properties and rotation characteristic of the nanofin [30–32]. Usually, the operator of the metasuface acted on the incident light is expressed as $M = R(-\theta) \cdot J \cdot R(\theta)$. $R(\theta)$ and J are the rotation matrix and birefringent Jones matrix respectively, expressed as follow [33,34]:

$$R(\theta) = \begin{bmatrix} \cos\theta & \sin\theta \\ -\sin\theta & \cos\theta \end{bmatrix}, \qquad J = \begin{bmatrix} e^{i\phi_x} & 0 \\ 0 & e^{i\phi_y} \end{bmatrix}, \tag{1}$$

where θ is the rotation angle of the nanofin. ϕ_x and ϕ_y are the delay phases along x and y directions, respectively. For the partial polarization conversion condition, two parts of light with different polarizations will coexist in the transmission. To construct a generalized framework for phase manipulation under an arbitrary polarization conversion condition, the evolutionary process of incident light after passing through the metasurface can be assumed as follows:

$$\begin{cases} M|\lambda^+\rangle = f_1|\lambda^-\rangle^* + f_2|\lambda^+\rangle^* \\ M|\lambda^-\rangle = f_3|\lambda^-\rangle^* + f_4|\lambda^+\rangle^* \end{cases}, \tag{2}$$

where $|\lambda^+\rangle$ and $|\lambda^-\rangle$ denote a pair of orthogonal states of polarization for the incident light. These f parameters are complex numbers that contain both amplitude and phase information, allowing for effective phase manipulation and energy distribution of each component. The physical process of light field transformation in Eqs. (2) can be easily and clearly clarified via the circularly polarized basis. When there is an arbitrarily polarized state $|\lambda^+\rangle$ incident on the metasurface, the component LCP (RCP) will be converted into one portion of LCP (RCP) with propagation phase modulation and RCP (LCP) with hybrid phase (propagation phase and geometric phase) modulation. These four items can perfectly interfere and be synthesized into the OCS $|\lambda^-\rangle^*$ and CCS $|\lambda^+\rangle^*$ with different complex amplitude modulations. Hence, both propagation phase and geometric phase play a vital role in the light manipulation of the proposed framework. (Detailed analysis can be found in Supplemental Material [35].) Utilizing the orthogonal and normal properties of the polarization states in the transmission, Eqs. (2) can be recast as (see Supplemental Material [35]):

$$\begin{cases} f_1 = \Lambda_1 \alpha \beta^* - \Lambda_2 \alpha^* \beta \\ f_2 = \alpha^2 \Lambda_1 + \beta^2 \Lambda_2 \\ f_3 = (\alpha^*)^2 \Lambda_2 + (\beta^*)^2 \Lambda_1 \\ f_4 = f_1 \end{cases}, \tag{3}$$

where Λ_1 and Λ_2 are the eigenvalues of the birefringent Jones matrix J with the values $e^{i\phi_x}$ and $e^{i\phi_y}$, respectively. α and β represent the projection of input polarization state $|\lambda^+\rangle$ onto the eigenvectors $|x_1\rangle$ and $|x_2\rangle$ of the M matrix, where $|x_1\rangle = \begin{bmatrix} \cos\theta \\ \sin\theta \end{bmatrix}$, $|x_2\rangle = \begin{bmatrix} -\sin\theta \\ \cos\theta \end{bmatrix}$. The parameter f_1 is equal to f_4, which results in the same information for the $C1$ and $C4$. The right-hand side of Eqs. (3) describes the basic characteristics of the nanofin such as phase delay (ϕ_x, ϕ_y) and rotation angle (θ) that can be engineered for realizing the desired target on the left. This provides a way for metasurface design suitable for the arbitrary polarization conversion condition. For the single-layer metasurface composed of unit cells, only three independent eigenstate phases exist including two independent propagation phases and one pair of mutually conjugate phases. These phases are mutually coupled, leading to an identical modulation information on the $C1$ and $C4$ polarization channels. Therefore, at most, three independent polarization channels can be effectively manipulated in this condition.

Note that three free parameters (Λ_1, Λ_2, and α or ϕ_x, ϕ_y, and θ) are available in the left side of Eq. (3) for metasurface engineering, while four free targets need to be satisfied. Therefore, the solvability of the equation is critical. When the incident light is completely converted to its CCS ($f_1 = f_4 = 0$, $|f_2| = |f_3| = 1$), only two targets need to be satisfied in Eqs. (3), making the equation mathematically solvable under this condition. When the incident light is completely converted to its OCS ($|f_1| = |f_4| = 1$, $f_2 = f_3 = 0$), only one target should be considered, and the equation is obviously solvable. However, when the incident light is partially converted into CCS (the parameters f are not equal to zero), the number of targets exceeds the number of free parameters. Although the exact solution does not exist in this case, the approximate solution with small deviations can be obtained by multiobjective optimization. The form of Eqs. (3) under different constraints are discussed in detail in Supplemental Material [35].

The elliptical polarization represents the most general case on the Poincaré sphere. To begin with, we demonstrate the independent phase control of three polarization channels for orthogonal elliptic polarized light. We designed, fabricated, and tested a metasurface (noted as sample 1) that encodes three independent holograms on channels $C1$, $C2$, and $C3$. The encoded phases profiles on the metasurface yield intensity images of two strings (CAS and Meta) and one Chinese character ("guang," means light), computed based on the iterative phase retrieval of the Fresnel diffraction [40]. For convenience, the absolute values of f_1 and f_3 are set as $\sqrt{2}/2$ to make sure the energy in each channel is the same. According to Eqs. (3), a metasurface consisting of rectangular Si nanofins was engineered to impose these phase profiles on the $C1$, $C2$, and $C3$, respectively. The operating wavelength is designed at $\lambda = 980$ nm. The finite-difference time domain (FDTD) method was implemented to identify the nanopillars whose phase response satisfied the requirements of Eqs. (3). The height of the pillars is 700 nm and the lattice distance is 550 nm. The metasurface was fabricated via electron-beam lithography. The experimental setup is shown in Fig. 2(a). The LP1 (QWP2) and QWP1 (LP2) are used for generating (selecting) the corresponding elliptically polarized light. As shown in Fig. 2(b), the corresponding holograms have been obtained when a different polarization channel is selected. Obviously, the differences between the design images and measured holograms are very slight. Additionally, the hologram of $C4$ is the same as that of $C1$, consistent with the conclusion that f_1 and f_4 have the equal value. These results clearly demonstrate that the proposed framework can achieve independent phase control of three polarization channels under the partial elliptic polarization conversion condition. (The detail design and simulation can be seen in Supplemental Material [35].)

Next, we will demonstrate that the proposed framework is also compatible with the previous tripolarization-channel phase control methods for the circular (or linear) polarization light. Two metasurfaces encoded three different spiral phases ($e^{2i\theta}$, $e^{i\theta}$, $e^{3i\theta}$) on the $C1$, $C2$, and $C3$ were designed for the case of the circular and linear polarization light (noted as samples 2 and 3, respectively). The absolute values of f_1 and f_3 are the same as above. The phase response of Si nanopillar in an arbitrary position of the metasurface can be effectively determined by Eqs. (3).

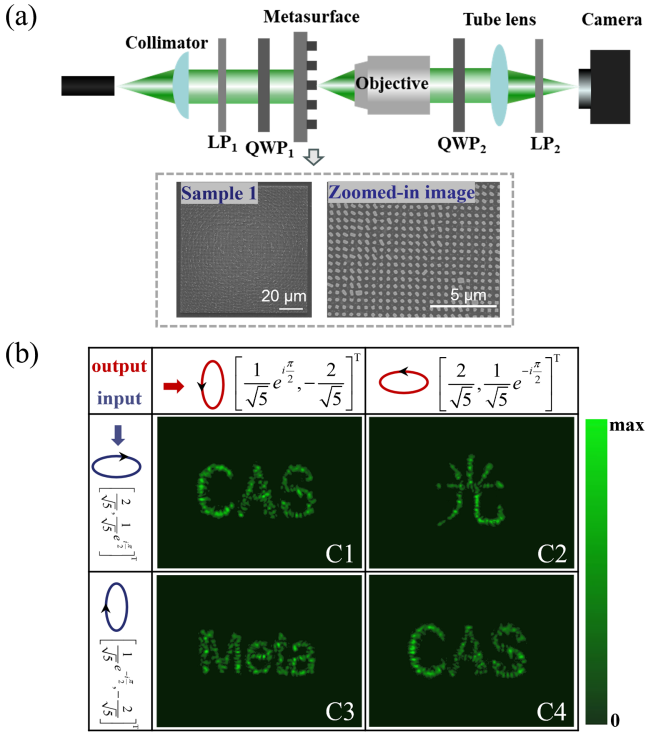

FIG. 2. (a) Experimental setup for measurement. The wavelength of the laser is 980 nm. LP1, LP2 are the linear polarizers. QWP1, QWP2 are the quarter wave plates. The LP1 and QWP1 are used for generated the incident elliptically polarized light. The LP2 and QWP2 are used for selecting the desired elliptically polarized light. (b) The holograms of different polarization channels.

The nanopillars were picked from the same database obtained using the FDTD method. The experimental setup is similar to the previous one. It is necessary to reset the polarizer and the wave plate to generate and select the corresponding circularly or linearly polarized light. The hollow ring intensities and fork interferograms for these two cases are shown in Fig. 3. Obviously, the numbers of the interference fringes (row 2 and row 4) are 2, 1, 3, and 2 from left to right, respectively, indicating that the experimental topological charges coincide with our design. Therefore, the proposed framework is also suitable for independent phase control in the partial circularly or linearly polarized conversion condition. For sample 2, the helical phases of $C1$ and $C4$ arise from the coupling of propagation phases, whereas those of $C2$ and $C3$ result from the interplay between geometric and propagation phases. Hence, only the light field evolution of $C2$ and $C3$ involves the spin-orbit interaction, and the corresponding incident light obtains OAM with the change of spin angular momentum. Additionally, to further validate the phase manipulation capabilities of the proposed metasurface, we conducted measurements of the surface phase of sample 2, and the results align well with the simulations. (See Supplemental Material for details [35].)

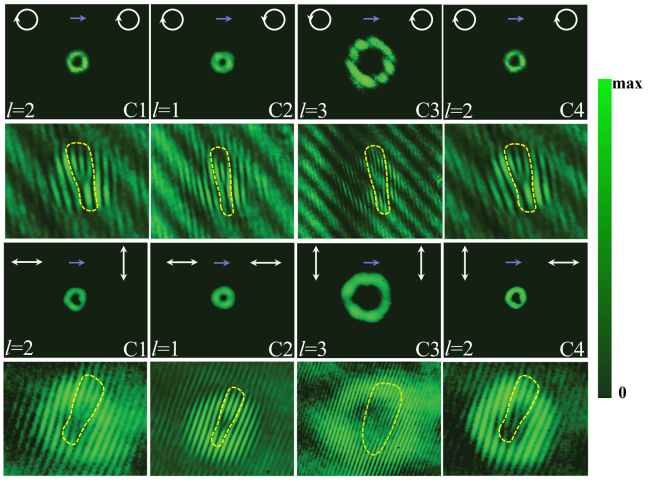

FIG. 3. Intensity distributions (top row) and fork interferograms (bottom row) for different polarization channels. The radius of the ring increases with the increase of the topological charge. The number of the interference fringes are 2, 1, 3, and 2 respectively, consist with the topological charge of the orbital angular momentum (OAM) beams.

The independent phase control for the linear, circular, elliptical polarized light has been realized in the partial polarized conversion condition. Next, we mainly demonstrate the arbitrary energy distribution control between the channels $C1$ and $C2$ (or $C3$ and $C4$) based the proposed framework. Without loss of generality, the case of elliptical polarization state is analyzed. Five metasurfaces (noted as sample I, sample II, sample III, sample IV, sample V in turn) were designed with the increasing polarization conversion efficiency in turn. They are encoded with the same focus phases on the $C1$, $C2$, and $C3$, which will generate three different focal points on the plane perpendicular to the propagation direction of the incident light. The required phase of Si nanopillars on the metasurface are obtained by the same method as above. The energy evolution process with the polarization conversion is shown in Fig. 4(a). With the increase of polarization conversion efficiency, the intensity of $C1$ ($C4$) increases, while the intensity of $C2$ ($C3$) decreases, which is consistent with our design. The deviations of theoretical energies and measured energies for different polarization channels are very slight, shown in Fig. 4(b). The total energy of $C1$ and $C2$ is close to 1 under the whole evolution process [Fig. 4(c)], which is due to the conservation of energy. These results indicate that the proposed framework can realize not only the phase manipulation but also the energy distribution for the different polarization channels, providing a more flexible and universal method for the light manipulation of metadevices. To further verify the wideband operational characteristics of the metasurface, the focusing properties of sample III within the incident wavelength range of 950 nm to 1020 nm have also been analyzed. The experiment demonstrates that the incident light can be well focused in

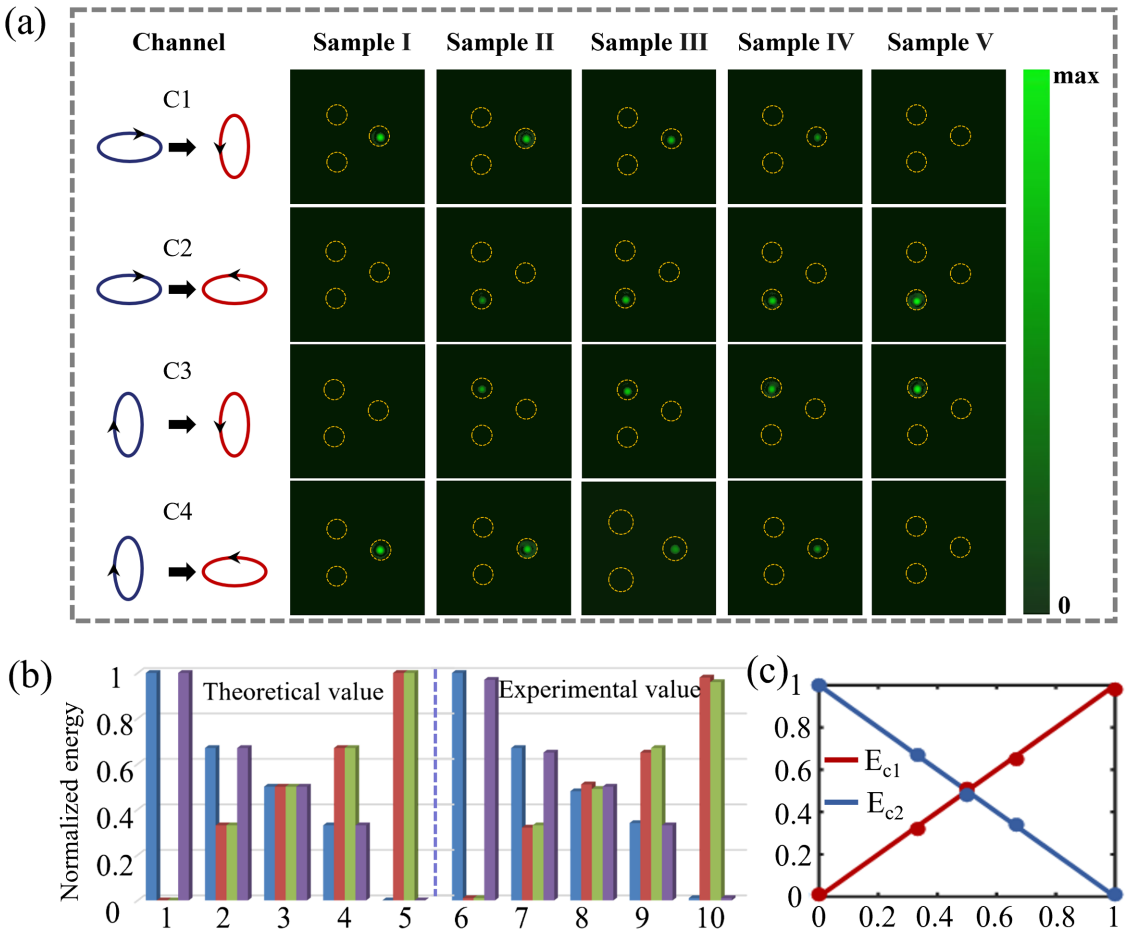

FIG. 4. The results of energy distribution manipulation based on the proposed framework. (a) Intensity distributions for different polarization conversion efficiencies. (b) The theoretical energies and measured energies for different polarization channels. (c) Energy evolution process for $C1$ and $C2$.

this wavelength range. Within the range of 60 nm, the relative focusing efficiency values are all greater than 0.88. Additionally, we also utilized sample III to explore its applications in the communications field, successfully achieving three-channel signal routing through the switching of polarization states. The detailed information is presented in Supplemental Material [35].

When the incident polarization state is completely converted into its complex conjugate state, only two polarization channels will remain for light manipulation, which degenerates into a previously reported case: independent phase control of arbitrary orthogonal states of polarization [10]. Here, the parameter f_1 is set to zero and information encoded on $C2$ and $C3$ is the strings (CAS) and the Chinese character (guang), and the fabricated metasurface is noted as sample 4. The incident polarization states are set as the same as that of the partial elliptic polarization conversion condition. As shown in Fig. 5, the information on $C2$ and $C3$ is consistent with our design. Besides, the intensities on $C1$ and $C4$ are very weak, which is also aligned with the theoretical expectation. Hence, the proposed framework is also compatible with light manipulation under the condition of complete polarization conversion.

In summary, we propose a generalized framework of phase manipulation for the metasurface-based polarization

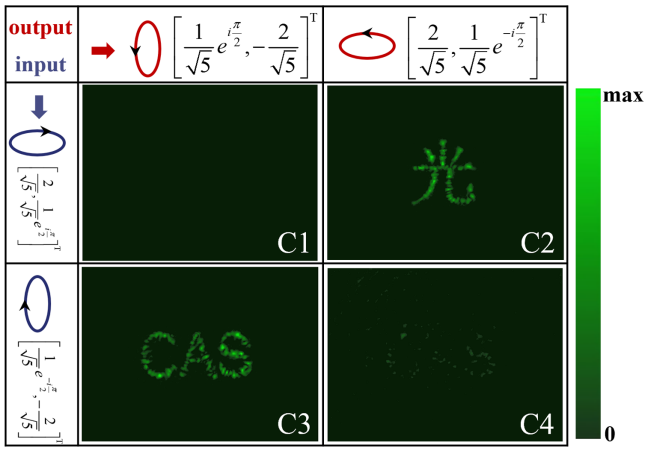

FIG. 5. The phase manipulation of elliptical polarization states for the complete polarization conversion condition.

optics under the condition of the arbitrary polarization state and arbitrary polarization conversion efficiency. The tripolarization-channel independent phase manipulation has been realized for the elliptically polarized, circularly polarized, and linearly polarized light in the partial polarization conversion condition. Besides, the energy distribution ratio between different channels can also be effectively controlled by the polarization conversion efficiency. Furthermore, independent phase manipulation of the orthogonal elliptical polarizations is shown to demonstrate that the proposed framework is also suitable for the case of complete polarization conversion. The proposed framework significantly improves the performance of metasurface in the polarization multiplexing and energy distribution, and extremely expands the application scope of metasurface in the polarization optics, providing a way toward engineering of novel polarization multiplexing metadevices.

Acknowledgments—The authors wish to acknowledge Junwei Min (Xi'an Institute of Optics and Precision Mechanics of Chinese Academy of Sciences), Yipeng Zheng (Xi'an University of Posts & Telecommunications), Peng Li (Northwestern Polytechnical University) for their help with the experimental measurement. Thanks to Xingyi Li (Zhejiang University) for his meaningful advice on our method. This work was supported by the National Natural Science Foundation of China (Grants No. 62205370, No. 62375282), the Youth Innovation Promotion Association of CAS (Grant No. J23-052-III), Natural Science Basis Research Plan in Shaanxi Province of China (Grant No. 2022JQ-047).

The authors Siqi Li and Chen Chen contributed equally to this work.

[1] A. H. Dorrah, N. A. Rubin, A. Zaidi, M. Tamagnone, and F. Capasso, Nat. Photonics **15**, 287 (2021).
[2] A. Arbabi and A. Faraon, Nat. Photonics **17**, 16 (2023).
[3] L. Huang, S. Zhang, and T. Zentgraf, Nanophotonics **7**, 1169 (2018).
[4] M. Xu, Q. He, M. Pu, F. Zhang, L. Li, D. Sang, and X. Luo, Adv. Mater. **34**, 2108709 (2022).
[5] Q. Fan, M. Liu, C. Zhang, W. Zhu, Y. Wang, P. Lin, and T. Xu, Phys. Rev. Lett. **125**, 267402 (2020).
[6] S. Wan, C. Wan, C. Dai, Z. Li, J. Tang, G. Zheng, and Z. Li, Adv. Opt. Mater. **9**, 2101547 (2021).
[7] J. Ji, J. Li, Z. Wang, X. Li, J. Sun, J. Wang, B. Fang, C. Chen, X. Ye, S. Zhu *et al.*, Nat. Commun. **15**, 8271 (2024).
[8] M. Khorasaninejad, W. T. Chen, R. C. Devlin, J. Oh, A. Y. Zhu, and F. Capasso, Science **352**, 1190 (2016).
[9] Y. Ni, S. Chen, Y. Wang, Q. Tan, S. Xiao, and Y. Yang, Nano Lett. **20**, 6719 (2020).
[10] J. B. Mueller, N. A. Rubin, R. C. Devlin, B. Groever, and F. Capasso, Phys. Rev. Lett. **118**, 113901 (2017).
[11] P. Huo, C. Zhang, W. Zhu, M. Liu, S. Zhang, S. Zhang, and T. Xu, Nano Lett. **20**, 2791 (2020).
[12] X. Li, Y. Zhou, S. Ge, G. Wang, S. Li, Z. Liu, and W. Zhang, Opt. Lett. **47**, 977 (2022).
[13] B. Wang, F. Dong, D. Yang, Z. Song, L. Xu, W. Chu, and Y. Li, Optica **4**, 1368 (2017).
[14] M. R. Akram, M. Q. Mehmood, X. Bai, R. Jin, M. Premaratne, and W. Zhu, Adv. Opt. Mater. **7**, 1801628 (2019).
[15] G. Zheng, H. Mühlenbernd, M. Kenney, G. Li, T. Zentgraf, and S. Zhang, Nat. Nanotechnol. **10**, 308 (2015).
[16] M. Pu, X. Li, X. Ma, Y. Wang, Z. Zhao, C. Wang, C. Hu, P. Gao, C. Huang, H. Ren *et al.*, Sci. Adv. **1**, e1500396 (2015).
[17] W. T. Chen, M. Khorasaninejad, A. Y. Zhu, J. Oh, R. C. Devlin, A. Zaidi, and F. Capasso, Light Sci. Appl. **6**, e16259 (2017).
[18] S. Li, X. Li, L. Zhang, G. Wang, L. Zhang, M. Liu, C. Zeng, L. Wang, Q. Sun, W. Zhao *et al.*, Adv. Opt. Mater. **8**, 1901666 (2020).
[19] Y. Guo, S. Zhang, M. Pu, Q. He, J. Jin, M. Xu, S. Zhang, and X. Luo, Light Sci. Appl. **10**, 63 (2021).
[20] H. Zhang, Z. Zhang, X. Ma, M. Pu, X. Li, Y. Guo, and X. Luo, Opt. Express **30**, 12069 (2022).
[21] M. Khorasaninejad, A. Y. Zhu, C. Roques-Carmes, W. T. Chen, J. Oh, I. Mishra, R. C. Devlin, and F. Capasso, Nano Lett. **16**, 7229 (2016).
[22] Y. Bao, L. Wen, Q. Chen, C.-W. Qiu, and B. Li, Sci. Adv. **7**, eabh0365 (2021).
[23] B. Xiong, Y. Liu, Y. Xu, L. Deng, C.-W. Chen, J.-N. Wang, R. Peng, Y. Lai, Y. Liu, and M. Wang, Science **379**, 294 (2023).
[24] Y. Bao, F. Nan, J. Yan, X. Yang, C.-W. Qiu, and B. Li, Nat. Commun. **13**, 7550 (2022).
[25] Y. Yuan, K. Zhang, B. Ratni, Q. Song, X. Ding, Q. Wu, S. N. Burokur, and P. Genevet, Nat. Commun. **11**, 4186 (2020).
[26] Y. Hu, L. Li, Y. Wang, M. Meng, L. Jin, X. Luo, Y. Chen, X. Li, S. Xiao, H. Wang *et al.*, Nano Lett. **20**, 994 (2019).
[27] H. Zhou, B. Sain, Y. Wang, C. Schlickriede, R. Zhao, X. Zhang, Q. Wei, X. Li, L. Huang, and T. Zentgraf, ACS Nano **14**, 5553 (2020).
[28] C. Chen, S. Gao, X. Xiao, X. Ye, S. Wu, W. Song, H. Li, S. Zhu, and T. Li, Adv. Photonics Res. **2**, 2000154 (2021).
[29] C. Chen, X. Xiao, X. Ye, J. Sun, J. Ji, R. Yu, W. Song, S. Zhu, and T. Li, Light Sci. Appl. **12**, 288 (2023).
[30] S. Li, X. Li, G. Wang, S. Liu, L. Zhang, C. Zeng, L. Wang, Q. Sun, W. Zhao, and W. Zhang, Adv. Opt. Mater. **7**, 1801365 (2019).
[31] Z. Guo, L. Zhu, F. Shen, H. Zhou, and R. Gao, RSC Adv. **7**, 9872 (2017).
[32] D. Lin, P.-Y. Fan, E. Hasman, and M. L. Brongersma, Science **345**, 298 (2014).
[33] A. Arbabi, Y. Horie, M. Bagheri, and A. Faraon, Nat. Nanotechnol. **10**, 937 (2015).
[34] N. A. Rubin, G. D'Aversa, P. Chevalier, Z. Shi, W.-T. Chen, and F. Capasso, Science **365**, eaax1839 (2019).
[35] See Supplemental Material at http://link.aps.org/supplemental/10.1103/PhysRevLett.134.023803 for detailed theoretical derivation of light manipulation and the

property analysis of the designed metasurface, which includes Refs. [10,36–39].

[36] C. Guan, J. Liu, X. Ding, Z. Wang, K. Zhang, H. Li, M. Jin, S. N. Burokur, and Q. Wu, Nanophotonics **9**, 3605 (2020).

[37] Y. Chen, X. Yang, and J. Gao, Light Sci. Appl. **7**, 84 (2018).

[38] Z. Maoxiong, C. M. Ku, Z. Ze-Peng, Y. Zhang, A. Chen, C. Qinmiao, W. Liu, J. Wang, C. Ze-Ming, B. Wang *et al.*, Light Sci. Appl. **10**, 52 (2021).

[39] S. M. Kamali, E. Arbabi, A. Arbabi, Y. Horie, and A. Faraon, Laser Photonics Rev. **10**, 1002 (2016).

[40] Z. Mou, X. Lu, H. Lv, Y. Han, Q. Yue, S. Wang, and S. Teng, Opt. Lasers Eng. **131**, 106146 (2020).